ARTICLES

Dielectric Relaxation Time and Relaxation Time Distribution of Alcohol−Water Mixtures

Seiichi Sudo, Naoki Shinyashiki,* Yusuke Kitsuki, and Shin Yagihara

Department of Physics, Tokai University, Hiratsuka, Kanagawa 259-1292, Japan

Received: August 10, 2001; In Final Form: October 29, 2001

Complex permittivity was measured in the frequency range from 10 MHz to 20 GHz at 25 °C for water mixtures of 22 aliphatic alcohols. The molecular structures of these alcohols systematically changed with the number of carbon atoms and hydroxyl groups, and their positions in the molecules. The asymmetric shape of the frequency dependence of the dielectric loss for the primary relaxation process was observed for each mixture. The broadness of the asymmetric dielectric loss depends on the water content, and the broadest dielectric loss was observed in the water mole fraction range of $0.65 < x_w < 0.85$. There is a strong correlation between the broadness of dielectric loss and the number of carbon atoms in the alcohol molecule. Deviations of observed relaxation times from those estimated for ideal mixtures depend on the number of carbon atoms except for the mixtures of water and alcohols with large alkyl groups, which form a micelle-like structure. These experimental results are interpreted on the basis of a model of three kinds of cooperative domains coexisting in the mixtures.

Introduction

The strong intermolecular interaction through hydrogen bonds in molecular liquids results in a peculiar dynamical property, compared with other simple liquids, as generally indicated in experimental results of dielectric measurements. Although the structures of water and associated monohydric alcohols are complicated due to molecular clusters and network structures through hydrogen bonds, the primary dielectric relaxation process exhibits a single Debye-type relaxation.[1−3] The dynamics of alcohol−water mixtures depending on the molecular structure of alcohol have also been studied by dielectric, calorimetric, and other experimental techniques.[4−20] The primary dielectric relaxation process is also observed for alcohol−water mixtures, but the complex permittivity with asymmetric shape of dielectric loss[8,11−13] has been generally described by the Kohlrausch−Williams−Watts (KWW) function,[13,21−23] the Havriliak−Negami (HN) equation,[8,11−13,24] or a sum of the Debye equations and/or the Cole−Cole equations.[4,5,9,10] The KWW function gives the complex permittivity as

$$\epsilon^*(\omega) = \epsilon_\infty + (\epsilon_0 - \epsilon_\infty)\int_0^\infty \left[-\frac{d\Phi(t)}{dt} \right] \exp(-j\omega t)\, dt \quad (1)$$

Here, $\Phi(t) = \exp[(-t/\tau)^{\beta_K}]$, where ϵ_0 is the limiting low-frequency permittivity, ϵ_∞ is the limiting high-frequency permittivity, τ is the relaxation time, ω is the angular frequency, and β_K ($0 < \beta_K \leq 1$) is a parameter for the asymmetrical broadness of the relaxation curve. The relaxation curve with $\beta_K = 1$ indicates the Debye-type relaxation. A smaller value of β_K gives a broader asymmetric relaxation curve. The HN equation gives the complex permittivity as

$$\epsilon^*(\omega) = \epsilon_\infty + \frac{\epsilon_0 - \epsilon_\infty}{[1 + (j\omega\tau)^\beta]^\alpha} \quad (2)$$

where α ($0 < \alpha \leq 1$) is a shape parameter used to express asymmetrical broadness of the relaxation curve, and β ($0 < \beta \leq 1$) is that for the symmetrical broadness. The parameters $\alpha = 1$ and $\beta = 1$ indicate the Debye-type relaxation, and the parameter $\alpha = 1$ indicates the Cole−Cole-type relaxation with the shape parameter β.

Only one relaxation peak is observed for many molecular liquid−water mixtures.[4−13] The broadness of the frequency dependence of the complex permittivity reflects the microscopic environments for dipoles through the rearrangement. Thus, these dielectric properties related to the relaxation time and its distribution offer important bindings to understand the molecular mechanism of dynamical liquid structures under molecular interaction. Although alcohol is the most popular material employed to study the hydrogen-bonding molecular liquids, it has been investigated systematically only for a few different alcohols.[4−20] In the present work, dielectric measurements of the mixtures of water and alcohol with 22 aliphatic alcohols were carried out in order to clarify the universal rules in dielectric relaxation time and the shape of the dielectric loss of alcohol−water mixtures.

Experiment

The aliphatic alcohols used in these experiments are listed in Table 1. Structures of these alcohols with various numbers

* Author to whom correspondence should be addressed.

10.1021/jp013117y CCC: $22.00
Published on Web 12/27/2001

TABLE 1: Various Molecular Structures Classified with Groups. Alcohols, Number of Carbon Atoms of Alcohol Molecule, N_C, Number of OH Groups, N_{OH}, and Number of C−C Bonds between OH Groups in Dihydric Alcohol, d_{OH}, Are Listed for Each Group

groups	alcohols	N_C	N_{OH}	d_{OH}
n-ol	methanol	1	1	
	ethanol	2	1	
	1-propanol	3	1	
s-ol	2-propanol	3	1	
	2-butanol	4	1	
12-diol	1,2-propanediol	3	2	1
	1,2-butanediol	4	2	1
	1,2-pentanediol	5	2	1
	1,2-hexanediol	6	2	1
EN-diol	1,3-butanediol	4	2	2
	1,4-pentanediol	5	2	3
	1,5-pentanediol	6	2	4
EE-diol	ethyleneglycol	2	2	1
	1,3-propanediol	3	2	2
	1,4-butanediol	4	2	3
	1,5-pentanediol	5	2	4
NN-diol	2,3-butanediol	4	2	1
	2,4-pentanediol	5	2	2
	2,5-hexanediol	6	2	3
triol	glycerol	3	3	
	1,2,4-butanetriol	4	3	
	1,2,6-hexanediol	6	3	

of carbon atoms, N_C, can be classified into seven characteristic groups on the basis of the different numbers of hydroxyl groups and the number of C−C bonds between the hydroxyl groups for the dihydric alcohols. Monohydric alcohols are also classified into two groups according to the position of the hydroxyl group, i.e., normal alcohols and secondary alcohols. The normal alcohols (n-ol) used are methanol, ethanol, and 1-propanol. The secondary alcohols (s-ol) used are 2-propanol and 2-buthanol. Dihydric alcohols can be classified into four groups according to the position of the hydroxyl groups, which are named to as 12-diol, EN-diol, EE-diol, and NN-diol. The hydroxyl groups of 12-diol are present on the terminal carbon atom and neighboring carbon atom (1,2-propanediol, 1,2-butanediol, 1,2-pentanediol, and 1,2-hexanediol). The hydroxyl groups of EN-diol are present on the carbon atom at one terminal and the second carbon atom from the opposite terminal carbon atom (1,3-butanediol, 1,4-pentanediol, and 1,5-hexanediol). The hydroxyl groups of EE-diol are present on the carbon atoms at the both terminals (ethyleneglycol, 1,3-propanediol, 1,4-butanediol, and 1,5-pentanediol). The hydroxyl groups of the NN-diol are present on the neighboring carbon atoms of both terminal carbon atoms (2,3-butanediol, 2,4-pentanediol, and 2,5-hexanediol). The trihydric alcohols (triol) used are glycerol, 1,2,4-butanetriol, and 1,2,6-hexanetriol. Ethyleneglycol was purchased from Wako Pure Chemical industries and other alcohols were purchased from Aldrich. Distilled and triple-deionized water with an electric conductivity lower than 18.3 μS/m was obtained by ultrapure water products (Millipore, MILLI-Q Lab). Alcohol−water mixtures in the concentration ranges of alcohol from 0 to 100 wt % at 10 wt % intervals, and 94 and 98 wt % were prepared.

The dielectric complex permittivity of alcohol−water mixtures was measured by time domain reflectometry (TDR) in the frequency range between 10 MHz and 20 GHz at 25 °C.

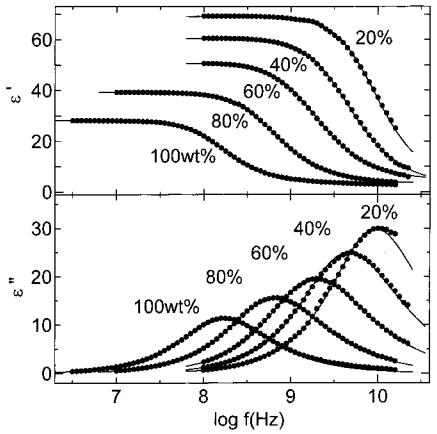

Figure 1. Dielectric constants and losses for mixtures of water and 1,3-butanediol at various concentrations at 25 °C. The solid line is calculated by the KWW function.

Details of the apparatus and the procedures of the TDR have been reported previously.[11,25,26]

Results & Discussion

Frequency Dependencies of the Complex Permittivities. Dielectric constants and losses for 20, 40, 60, 80, and 100 wt % 1,3-butanediol−water mixtures at 25 °C are shown in Figure 1. A single relaxation peak is observed for the entire concentration range of all the alcohol−water mixtures. The peak frequency shifts to a lower frequency with increasing alcohol concentration, and it reaches that for the pure alcohol. This dependency implies that the relaxation observed for the mixtures is due to rotational diffusive motion of both water and alcohol molecules.

We performed a curve fitting procedure for the frequency dependence of the complex permittivity for all the mixtures to determine relaxation parameters of the KWW function. The solid lines shown in Figure 1 were calculated from the KWW function. The frequency dependences of complex permittivity for 1,3-butanediol−water mixtures are described well by the KWW function in the entire concentration range. The error in the value of β_K was less than ± 0.03 for $0.95 \leq \beta_K \leq 1$ and ± 0.01 for $\beta_K < 0.95$. The frequency dependencies of the complex permittivity for the other mixtures of water and alcohol with four carbon atoms or less are described well by the KWW function in the entire concentration range the same as those of the 1,3-butanediol−water mixtures.

The shapes of the frequency dependence of the complex permittivity obtained for the mixtures of water and alcohol with five and six carbon atoms are different from those with four carbon atoms or less. The dielectric constants and losses for 20, 60, and 80 wt % 1,2-hexanediol−water mixtures are shown in Figure 2, parts a−c, respectively, as examples of the frequency dependence of the complex permittivity for the mixtures of water and alcohol with five carbon atoms or more. The solid, dashed, and dotted lines are calculated by the KWW function, HN equation, and sum of the Cole−Cole and Debye equations, respectively. The frequency dependencies of the complex permittivities for the 10, 20, and 80−100 wt % 1,2-hexanediol−water mixtures are well described by the KWW function within the frequency range of ± 1 decades at around the relaxation peak frequency shown in Figure 2, parts a and c, respectively. On the other hand, the frequency dependence of the complex permittivity for the 60 wt % 1,2-hexanediol−water mixture shown in Figure 2b can be described by the KWW function within the frequency range between $+1$ and -0.5

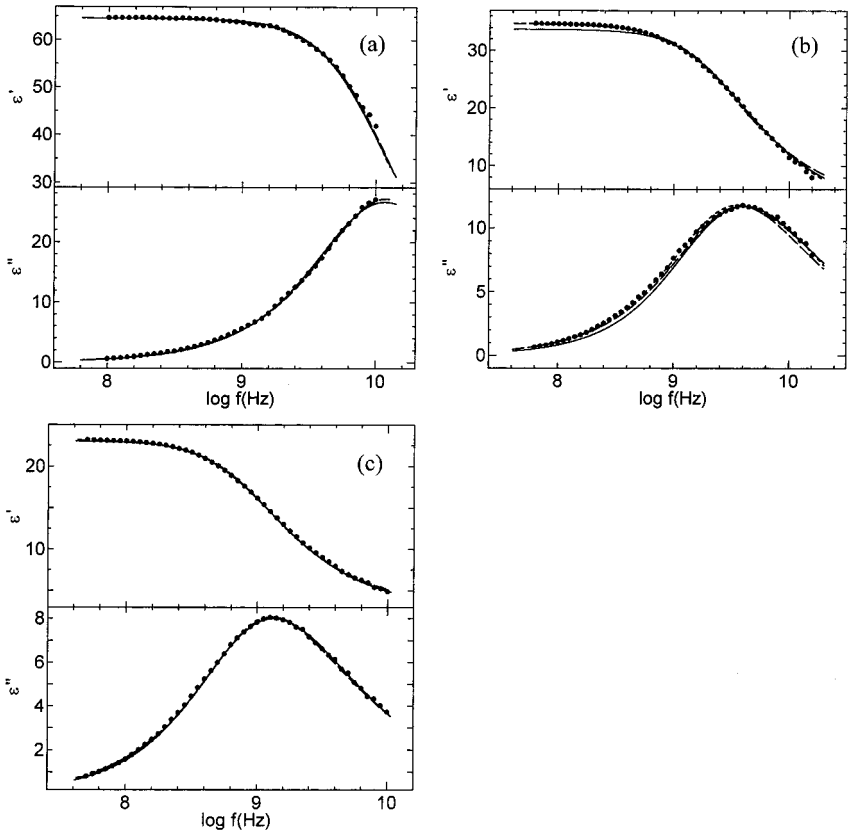

Figure 2. Dielectric constants and losses for the (a) 20, (b) 60, and (c) 80 wt % 1,2-hexanediol−water mixtures at various concentrations at 25 °C. The solid, dashed, and dotted lines are calculated by the KWW function, the HN equation, and sum of the Cole−Cole and Debye equations, respectively.

decades at around the peak frequency. If the dielectric loss is fitted by the KWW function only, the dielectric constant and loss in the frequency range lower than the relaxation peak frequency cannot be described, and the calculated dispersion curve is not reasonable. The value of the relaxation strength became larger due to the fitting in the lower-frequency range in the dielectric loss, and it is reflected that the value of ϵ_∞ becomes less than unity in the dispersion curve. The value of ϵ_∞ for the alcohol−water mixtures generally takes a value of $2-5$[4,8−12] and it should be larger than unity. The frequency dependence of the complex permittivity for the 30−70 wt % 1,2-hexanediol−water mixtures are also described by the KWW function in the frequency range between +1 and −0.5 decades at around the peak frequency. These frequency dependences of the complex permittivity for the mixtures of water and alcohols with five carbon atoms or more are well described by the HN equation or the sum of the Cole−Cole and Debye equations. In general, the frequency dependence of the complex permittivity for alcohol−water mixtures was described well by the HN equation and the sum of the Cole−Cole and Debye equations.[4,5,9−13] However, the broadness of the dielectric loss cannot be discussed easily on the basis of the HN equation or the sum of the Debye and Cole−Cole equations, because these equations require more than two parameters only to describe the broadness of the relaxation curve. On the other hand, the KWW function can explain the broadness with only one parameter, and the relaxation time and the broadness of the relaxation curve is evaluated accurately. In the present work, we performed the fitting procedure with the KWW function in order to simplify the discussions on the relaxation time and broadness of dielectric loss, and β_K is employed to compare the broadness of the dielectric loss for water mixtures with various alcohols and alcohol concentrations.

The asymmetric dielectric loss is interpreted with a heterogeneous structure such as the variation of the size and dynamical structure of a cooperative domain (CD).[27] The CD is defined as a domain in which the reorientation of molecules cooperatively occurs with dipole correlations. Then cooperative motion can be evaluated by the size and structure of CD. Stronger interactions among the moving units can yield a larger CD, and a variation of the size of the CD results in a corresponding variation of the microscopic relaxation time; this distribution of microscopic relaxation time exhibits an asymmetric dielectric loss. It has been reported that the asymmetric dielectric loss is interpreted by the model, in which the three types of microscopic dynamical environments coexist in a binary mixture of liquids.[24,28] According to the model in these reports, we assumed three kinds of CD in the alcohol−water mixtures in our previous study;[24] CD_W includes only water molecules, CD_A includes only alcohol molecules, and CD_{W-A} includes both water and alcohol molecules, and it was indicated that the composition of the each CD depends on the concentration and the molecular structure of alcohol. The dielectric behavior of the alcohol−water mixtures strongly reflects the size and fraction of CD_{W-A}, since the alcohol molecules cooperatively rearrange with the surrounding water molecules with which they interact through hydrogen bonds and/or clathrate-like hydrate aggregates. This model of the cooperative domain is introduced to discuss the relaxation time and the asymmetrical broadness of the dielectric loss in the following sections.

Relaxation Time. Figure 3 shows an example of the dependence of the relaxation time, τ_{obs}, on mole fraction of

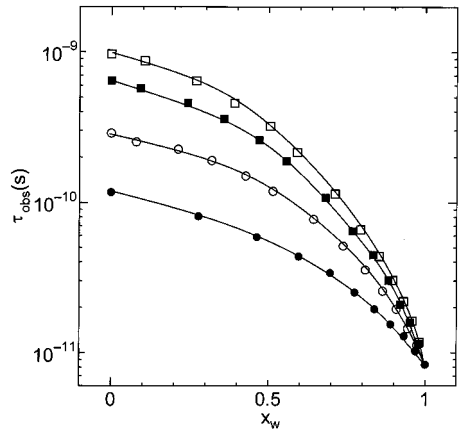

Figure 3. Dependence of the relaxation time, τ_{obs}, on mole fraction of water, x_w, for EE-diol−water mixtures at 25 °C. (●) Ethyleneglycol; (○) 1,3-propanediol; (■) 1,4-butanediol; (□) 1,5-pentanediol.

water, x_w, obtained from the curve fitting procedures with the KWW function for EE-diol−water mixtures. The τ_{obs} value decreases with increasing x_w. The x_w dependence of the logarithm of τ_{obs} is related to the apparent activation energy of the rearrangement of dipoles by the Eyring formula,[29]

$$\tau = \frac{h}{kT}\exp\left(\frac{\Delta G}{RT}\right) \tag{3}$$

where h is the Planck constant, k is the Boltzmann constant, T is the absolute temperature, R is the gas constant, and ΔG is the apparent activation free energy. Assuming an ideal mixture with liquid 1 and liquid 2 in which the dynamical structure of each pure liquid is retained, the apparent activation free energy, ΔG_{mix}, is given by

$$\Delta G_{mix} = x\Delta G_1 + (1-x)\Delta G_2 \tag{4}$$

where ΔG_1 and ΔG_2 are the apparent activation free energies for liquid 1 and liquid 2, respectively, and x is the mole fraction of liquid 1. An ideal behavior of the relaxation time, τ_{ideal}, for the mixture is then given by

$$\tau_{ideal} = \frac{h}{kT}\exp\left(\frac{\Delta G_{mix}}{RT}\right) = \tau_1^{\,x}\tau_2^{\,(1-x)} \tag{5}$$

This equation gives a linear dependence of the plots of logarithm of τ_{ideal} vs x. On the other hand, if ΔG_{mix} for these mixtures is given by the three kinds of free energies ΔG_1, ΔG_2, and ΔG_{12}, the observed relaxation time disagrees with eq 5, where ΔG_{12} is the apparent activation free energy of the mixed environment of molecules of liquid 1 and liquid 2. In addition, the relaxation time can be described by eq 5, if ΔG_{mix} is written as[28]

$$\Delta G_{12} = \frac{\Delta G_1 + \Delta G_2}{2} \tag{6}$$

Equation 6 implies that the free energy of the mixed environment is equal to the arithmetical mean of the free energies of the pure liquids.

A relationship between observed relaxation time, τ_{obs}, and τ_{ideal} was discussed in detail for various cases on the basis of the results of dielectric measurements:[11,28] weakly associated binary mixtures (chloroform− and aniline−acetone mixtures), normal alcohol−normal alcohol mixtures, normal alcohol−water mixtures, and nonassociated liquid−associated liquid mixtures. In refs 11 and 28, it was reported that the τ_{obs} for the normal

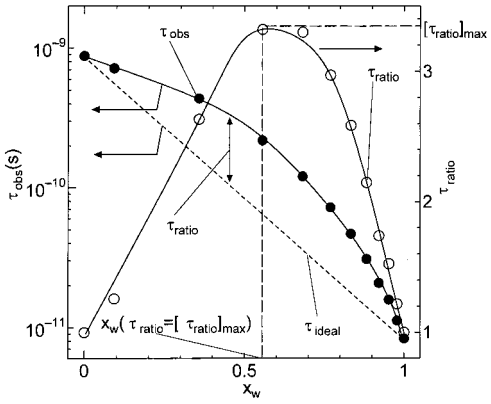

Figure 4. Dependence of the relaxation time, τ_{obs}, on mole fraction of water, x_w, for 1,3-butanediol−water mixtures at 25 °C (closed symbols). The dotted line shows the behavior for the ideal situation. The ratio of the observed relaxation time, τ_{obs}, and relaxation time of the ideal mixture, τ_{ideal} against x_w were shown by open symbols. The solid line for τ_{ratio} is a guide to the eyes.

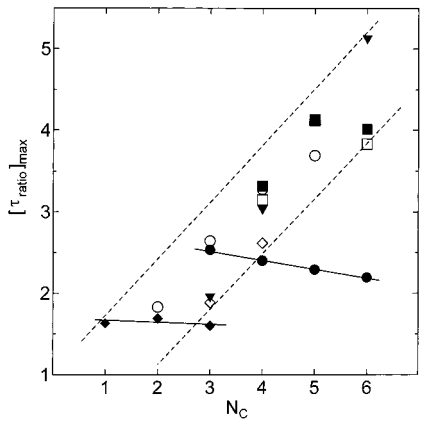

Figure 5. Plots of the maximum values of τ_{ratio}, $[\tau_{ratio}]_{max}$, against the number of carbon atoms, N_C, of alcohol molecule for all the mixtures. (◆) n-ol; (◇) s-ol; (●) 12-diol; (■) EN-diol; (○) EE-diol; (□) NN-diol; (▼) triol.

alcohol−normal alcohol mixtures completely agreed with τ_{ideal} for the entire concentration range. The value of τ_{obs} disagreed with that of τ_{ideal} for other mixtures. The ideal behavior arises in the case that the same type of intermolecular interaction occurs in the pure liquids and their mixture. These agreements between τ_{ideal} and τ_{obs} were explained by a similar dynamical structure in the normal alcohol mixtures, in which it is reasonable to assume that no significant structural change occurs with respect to the pure components.[28] These systems can be essentially ideal associated mixtures.

Figure 4 shows the plot of observed relaxation time, τ_{obs}, against x_w for the 1,3-butanediol−water mixture. Values of τ_{obs} and τ_{ideal} are given by the closed circles and the dotted line, respectively. The τ_{obs} values disagree with τ_{ideal} in the entire concentration range. To discuss the disagreement, τ_{ratio} is defined as the ratio τ_{obs}/τ_{ideal}. The τ_{ratio} values are represented by open circles and exhibit a maximum at $x_w \cong 0.6$ as shown in Figure 4. For all the alcohol−water mixtures measured, the same concentration dependence of the relaxation time is obtained and τ_{ratio} shows a maximum at $0.55 < x_w < 0.75$. Figure 5 shows a dependence of the maximum value of τ_{ratio}, $[\tau_{ratio}]_{max}$, on the number of carbon atoms of the alcohol molecule, N_C, for all the mixtures. The value of $[\tau_{ratio}]_{max}$ increases with increasing N_C except for n-ol and 12-diol. On the other hand, the $[\tau_{ratio}]_{max}$ values of n-ol and 12-diol slightly decrease with increasing N_C.

A x_w dependence of the τ_{ratio} of the alcohol−water mixtures can be discussed using the three kinds of CD, CD_W, CD_A, and CD_{W-A}. If the alcohol−water mixtures are ideal binary liquids, their ΔG_{mix} will be given by

$$\Delta G_{mix} = x_w \Delta G_W + (1 - x_w)\Delta G_A \quad (7)$$

where ΔG_W and ΔG_A are the apparent activation free energies of the rearrangement of CD_W and CD_A, respectively, and ΔG_{mix} denotes the average of ΔG_W and ΔG_A. The disagreement between the τ_{obs} and τ_{ideal} reflects the apparent activation free energy of the rearrangement of CD_{W-A}, ΔG_{W-A}. The mole fraction of water, $x_w(\tau_{ratio} = [\tau_{ratio}]_{max})$, where τ_{ratio} shows the maximum value, results from the largest contribution of ΔG_{W-A}.

Computer simulation in molecular dynamics studies suggests that upon adding hydrophobic molecules to a water system, the water molecules form clathrate-like hydrate aggregates around the hydrophobic molecule, stabilizing the hydrogen bond among these water molecules.[30,31] The formations of the clathrate-like hydrate aggregates or the cage structure of water molecules around each *tert*-butyl alcohol molecule and 2-propanol molecule also investigated by small-angle X-ray scattering.[32−35] The mixing state of the 1-propanol−water mixture is different from that of the *tert*-butyl alcohol−water mixture, and a 1-propanol molecule cannot be caged by water molecules,[35] because of the larger hydrophobic interaction in 1-propanol molecules. It was proposed that 1-propanol molecules form a micelle-like structure in the 1-propanol−water mixture by light scattering.[36] It is also reported, on the basis of a Monte Carlo simulation study, that chains consisting of two hydrophilic particles and five hydrophobic particles form a micelle-like structure.[37] These studies suggest that water molecules form clathrate-like hydrate aggregates around the alkane of the large alcohol molecule. We assumed that such water molecules simultaneously relaxing with the alcohol molecule form CD_{W-A} with the alcohol molecule. It is reasonable to consider that the CD_{W-A} in the larger alcohol−water mixtures is larger than that in the smaller alcohol−water mixture. The rearrangement of the larger CD_{W-A} requires the larger apparent activation free energy, which is reflected by the larger microscopic relaxation time. Therefore, $[\tau_{ratio}]_{max}$ depends on N_C in alcohol−water mixtures except for the 12-diol− and n-ol−water mixtures. On the other hand, independence of $[\tau_{ratio}]_{max}$ from N_C shown for n-ol− and 12-diol−water mixtures implies that the fraction of CD_{W-A} of these mixtures is smaller than that of other mixtures. The n-ol and 12-diol molecules have a relatively large alkane group and these molecules form a micelle-like structure in these water mixtures as has been previously reported.[35−37] These alcohol molecules forming a micelle-like structure move cooperatively with few water molecules, because the water molecules cannot form clathrate-like aggregates for the alkane of the alcohol molecule. The formation of the micelle-like structure of alcohol molecules avoids molecules constructing CD_{W-A}, if it is compared to mixtures of alcohol with the clathrate-like hydrate aggregation. Therefore, $[\tau_{ratio}]_{max}$ of the 12-diol− and n-ol−water mixtures are smaller than that of other alcohol−water mixtures with the clathrate-like hydrate aggregates. The dependence of the $[\tau_{ratio}]_{max}$ on the molecular structure of alcohol in alcohol−water mixtures is explained by the cooperative domain model, in terms of the formation of the CD_{W-A}, since alcohol and water molecules interact through hydrogen bonds and/or clathrate-like hydrate aggregates.

Broadness of Dielectric Loss. Figure 6 shows examples of x_w dependence of β_K for EE-diol−water mixtures. The values of β_K for all the mixtures decrease steeply with decreasing x_w for $0.9 < x_w$, and increase with decreasing x_w for $x_w < 0.6$. The minimum of β_K, $[\beta_K]_{min}$, indicates the broadest dielectric loss was observed at $0.65 < x_w < 0.85$ for each mixture. Figure 7 shows N_C dependence of $[\beta_K]_{min}$. The $[\beta_K]_{min}$ value decreases with increasing N_C for all the mixtures.

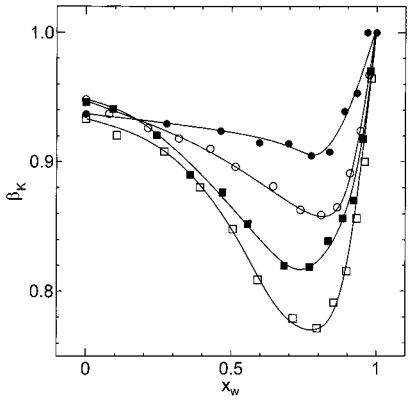

Figure 6. Dependence of the shape parameter for the asymmetric broadening, β_K, on x_w for EE-diol−water mixtures at 25 °C. (●) Ethyleneglycol; (○) 1,3-propanediol; (■) 1,4-butanediol; (□) 1,5-pentanediol.

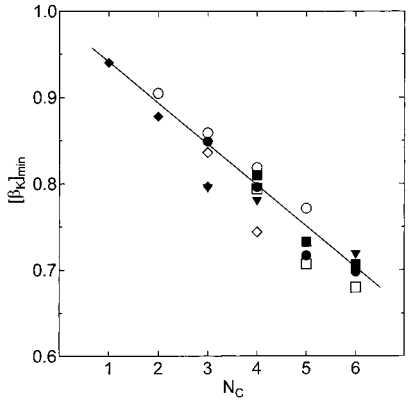

Figure 7. Plots of the minimum values of β_K, $[\beta_K]_{min}$, against the number of carbon atoms, N_C, of alcohol molecule for all the mixtures. (◆) n-ol; (◇) s-ol; (●) 12-diol; (■) EN-diol; (○) EE-diol; (□) NN-diol; (▼) triol.

Theoretical approaches for the shape of the relaxation curve suggest that the distribution of relaxation time originates from the cooperative motion of moving units.[27,38] Each CD has a different microscopic relaxation time reflecting each local environment. Then, if there is only one CD size, the same microscopic relaxation time of CD shows the Debye-type relaxation curve. In the case that the system has a variation of CD size, the relaxation curve shows an asymmetric shape due to the distribution of the microscopic relaxation time of CD. According to the cooperative domain model with three kinds of CD, CD_W, CD_A, and CD_{W-A}, the CD_W size is homogeneous, because of the Debye-type relaxation process for pure water. The CD_A size is heterogeneous, since the dielectric loss for many pure alcohols shows an asymmetric broadening. It can be expected that the variation of the CD_{W-A} size is larger than those of CD_W and CD_A size because of the fluctuation of microscopic concentration. The CD size in the alcohol−water mixtures is more heterogeneous than that in pure alcohol because the three kinds of CD coexist in the alcohol−water mixtures.

When alcohol is added to pure water, the alcohol molecules and the surrounding water molecules form CD_{W-A}. In $x_w(\beta_K = [\beta_K]_{min}) < x_w \leq 1$, i.e., the water-rich region, the fraction of CD_W decreases and that of CD_{W-A} increases with increasing

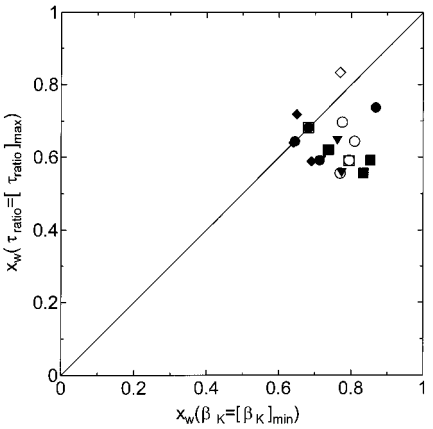

Figure 8. Plots of the mole fraction of water with the maximum value of τ_{ratio}, $x_w(\tau_{ratio} = [\tau_{ratio}]_{max})$, against the mole fraction of water with the minimum value of β_K, $x_w(\beta_K = [\beta_K]_{min})$. The solid line indicates $x_w(\tau_{ratio} = [\tau_{ratio}]_{max}) = x_w(\beta_K = [\beta_K]_{min})$. (◆) n-ol; (◇) s-ol; (●) 12-diol; (■) EN-diol; (○) EE-diol; (□) NN-diol; (▼) triol.

alcohol concentration, where $x_w(\beta_K = [\beta_K]_{min})$ is x_w at a minimum value of β_K. At $x_w(\beta_K = [\beta_K]_{min})$, the coexistence of CD_W, CD_{W-A}, and CD_A with certain fractions bring about $[\beta_K]_{min}$, i.e., the variation of the CD size is maximum. In $0 \le x_w < x_w(\beta_K = [\beta_K]_{min})$, the fraction of CD_A increases and those of CD_{W-A} and CD_W decrease with increasing alcohol concentration.

The $[\beta_K]_{min}$ value depends on N_C as shown in Figure 7. As we have already discussed, the larger alcohol−water mixtures have larger CD_{W-A} and larger microscopic relaxation times than smaller alcohol−water mixtures. The larger difference between the microscopic relaxation time of CD_{W-A} and CD_W results in a smaller value of $[\beta_K]_{min}$ for the larger alcohol−water mixtures, compared with that of the smaller alcohol−water mixtures. Rupprecht et al.[39] also suggested that the heterogeneous local structure studied by ultrasonic absorption spectra for various aqueous systems is related to the number of carbon atoms of solute, i.e., the size of alkyl chain of monohydric alcohols, poly(ethyleneglycol)monoalkyl ethers, and urea and its derivatives.

Although the exceptional behavior is clearly observed for $[\tau_{ratio}]_{max}$ in n-ol− and 12-diol−water mixtures, it is not observed for $[\beta_K]_{min}$. For the 12-diol− and n-ol−water mixtures, the fraction of CD_{W-A} is smaller than that for other alcohol−water mixtures, since alcohol molecules involved in micelle-like structure form the cooperative domain CD_A. However, even in this case, the difference between the microscopic relaxation times of the CD_W and that of the micelle-like structure CD_A results in small $[\beta_K]_{min}$.

Comparison of the Mole Fraction of Water at $[\beta_K]_{min}$ and $[\tau_{ratio}]_{max}$. As the physical significance of $[\beta_K]_{min}$ and $[\tau_{ratio}]_{max}$ is different, $x_w(\tau_{ratio} = [\tau_{ratio}]_{max})$ and $x_w(\beta_K = [\beta_K]_{min})$, appear at different x_w values. Figure 8 shows plots of $x_w(\tau_{ratio} = [\tau_{ratio}]_{max})$ against $x_w(\beta_K = [\beta_K]_{min})$ for all the mixtures. If $x_w(\tau_{ratio} = [\tau_{ratio}]_{max})$ and $x_w(\beta_K = [\beta_K]_{min})$ are same, these plots lie on the solid line. The values of $x_w(\tau_{ratio} = [\tau_{ratio}]_{max})$ and $x_w(\beta_K = [\beta_K]_{min})$ for all the mixtures are observed for $0.55 < x_w(\tau_{ratio} = [\tau_{ratio}]_{max}) < 0.75$ and $0.65 < x_w(\beta_K = [\beta_K]_{min}) < 0.85$, respectively. It is roughly shown that $x_w(\beta_K = [\beta_K]_{min})$ is obtained in a more water-rich region than $x_w(\tau_{ratio} = [\tau_{ratio}]_{max})$. It is reasonable to consider that the concentration range can be separated in three regions by $x_w(\beta_K = [\beta_K]_{min})$ and $x_w(\tau_{ratio} = [\tau_{ratio}]_{max})$ on the basis of the fractions of the three kinds of CD. In $x_w(\beta_K = [\beta_K]_{min}) < x_w \le 1$, CD_W decreases and CD_{W-A} increases with increasing alcohol concentration. The variation of the CD size of CD_W and CD_{W-A} or CD_A in the mixtures is the largest at $x_w(\beta_K = [\beta_K]_{min})$. In $x_w(\tau_{ratio} = [\tau_{ratio}]_{max}) < x_w < x_w(\beta_K = [\beta_K]_{min})$, CD_W decreases and CD_{W-A} and CD_A increase with increasing alcohol concentration. The τ_{ratio} value exhibits a maximum at $x_w(\tau_{ratio} = [\tau_{ratio}]_{max})$ because of the maximum contribution of ΔG_{W-A} and vanishing CD_W. In $0 \le x_w < x_w(\tau_{ratio} = [\tau_{ratio}]_{max})$, both the size and the fraction of CD_{W-A} decrease and the fraction of CD_A increases with increasing alcohol concentration. A few alcohol−water mixtures exhibit $x_w(\tau_{ratio} = [\tau_{ratio}]_{max}) \ge x_w(\beta_K = [\beta_K]_{min})$. However, the x_w dependence of $[\tau_{ratio}]$ is not sufficiently large to determine $[\tau_{ratio}]_{max}$ precisely.

Conclusions

Asymmetric dielectric losses are observed for mixtures of water and 22 aliphatic alcohols at various concentrations. Each mixture shows the minimum β_K value and the maximum τ_{ratio} value at certain concentrations. The $[\beta_K]_{min}$ value depends mainly on N_C and it decreases with increasing N_C. The mixtures of water with larger alcohols provide more heterogeneous local structure of CD_{W-A} and CD_W. $[\tau_{ratio}]_{max}$ is introduced to discuss the local structure of mixed environment, CD_{W-A}, and the $[\tau_{ratio}]_{max}$ value increases with increasing N_C for all the mixtures except for n-ol− and 12-diol−water mixtures. $[\tau_{ratio}]_{max}$ for n-ol− and 12-diol−water mixtures is smaller than that for other mixtures. This is probably due to the situation that the mixtures of water and 1-ol and larger 12-diol form micelle-like structure of alcohol molecules.

References and Notes

(1) Hasted, J. B. *Water, A Comprehensive Treatise*; Franks, F., Ed.; Plenum: New York, 1972; Chapter 7.
(2) Kaatze, U. *J. Chem. Eng. Data* **1989**, *34*, 371.
(3) Barthel, J.; Bachhuber, K.; Buchner, R.; Hetzenauer, H. *Chem. Phys. Lett.* **1990**, *165*, 369.
(4) Wang, F.; Pottel, R.; Kaatze, U. *J. Phys. Chem.* B **1997**, *101*, 922.
(5) Bao, J.; Swicord, M. L.; Davis, C. C. *J. Chem. Phys.* **1996**, *104*, 4441.
(6) Gestblom, B.; Sjöblom, J. *J. Phys. Chem.* **1986**, *90*, 4175.
(7) Takei, T.; Amano, C.; Nishimoto, Y.; Sugitani, Y. *Anal. Sci.* **1987**, *13*, 1043.
(8) Sato, T.; Niwa, H.; Chiba, A.; Nozaki, R. *J. Chem. Phys.* **1998**, *108*, 4138.
(9) Sato, T.; Chiba, A.; Nozaki, R. *J. Chem. Phys.* **1999**, *110*, 2508.
(10) Sato, T.; Chiba, A.; Nozaki, R. *J. Chem. Phys.* **2000**, *112*, 2924.
(11) Mashimo, S.; Umehara, T.; Redlin, H. *J. Chem. Phys.* **1991**, *95*, 6257.
(12) Mashimo, S.; Kuwabara, S.; Yagihara, S.; Higasi, K. *J. Chem. Phys.* **1989**, *90*, 3292.
(13) Shinyashiki, N.; Sudo, S.; Abe, W.; Yagihara, S. *J. Chem. Phys.* **1998**, *109*, 9843.
(14) Pflug, H. D.; Pope, A. E.; Benson, G. C. *J. Chem. Eng. Data* **1968**, *13*, 409.
(15) Pal, A.; Singh, Y. P. *J. Chem. Eng. Data* **1996**, *41*, 1008.
(16) Nikam, P. S.; Jadhav, M. C.; Hasan, M. *J. Chem. Eng. Data* **1996**, *41*, 1028.
(17) Aucejo, A.; Burguet, M. C.; Munoz, R. M. *J. Chem. Eng. Data* **1996**, *41*, 1131.
(18) Paduano, L.; Sartori, R.; D'Errico, G.; Vitagliano, V. *J. Chem. Soc., Faraday Trans.* **1998**, *94*, 2571.
(19) Lee, D. J.; Huang, W. H. *Colloid Polym. Sci.* **1996**, *274*, 160.
(20) Taniewska-Osińska, S.; Pietrzak, A. *Fluid Phase Equilib.* **1997**, *137*, 229.
(21) Kohlrausch, R. *Prog. Ann. Phys.* **1854**, *91*, 179.
(22) Williams, G.; Watts, D. C. *Trans. Faraday Soc.* **1971**, *66*, 80.
(23) Shinyashiki, N.; Yagihara, S. *J. Phys. Chem.* B **1998**, *103*, 4481.
(24) Havriliak, S.; Negami, S. *Polymer* **1963**, *8*, 9874.
(25) Mashimo, S.; Miura, N.; Umehara, T.; Yagihara, S.; Higasi, K. *J. Chem. Phys.* **1992**, *96*, 6358.
(26) Mahimo, S.; Miura, N. *J. Chem. Phys.* **1993**, *99*, 9874.
(27) Matsuoka, S. *J. Res. Natl. Inst. Stand. Technol.* **1997**, *102*, 213.
(28) Bertolini, D.; Cassettari, M.; Ferrari, C.; Tombari, E. *J. Chem. Phys.* **1998**, *108*, 6416.

(29) Hill, N. E.; Vaughan, W. E.; Price, A. H.; Davies, M. *Dielectric Properties and Molecular Behaviour*; Reinhold: London, 1969.
(30) Geiger, A.; Rahman, A.; Stillinger, H. *J. Chem. Phys.* **1979**, *70*, 263.
(31) Pangali, C.; Rao, M.; Berne, J. *J. Phys. Chem.* **1979**, *71*, 2982.
(32) Nishikawa, K.; Kodera, Y.; Iijima, T. *J. Phys. Chem.* **1987**, *91*, 3694.
(33) Nishikawa, K.; Hayashi, H.; Iijima, T. *J. Phys. Chem.* **1989**, *93*, 6559.
(34) Nishikawa, K.; Iijima, T. *J. Phys. Chem.* **1990**, *94*, 6227.
(35) Hayashi, H.; Nishikawa, K.; Iijima, T. *J. Phys. Chem.* **1990**, *94*, 8334.
(36) Groβmann, G. H.; Ebert, K. H. *Ber. Bunsen-Ges. Phys. Chem.* **1981**, *85*, 1026.
(37) Bhattacharya, A.; Mahanti, S. D.; Chakrabarti, A. *J. Chem. Phys.* **1998**, *108*, 10281.
(38) Ngai, K. L.; Rendell, R. W.; Rajagopal, K. A.; Teitler, S. *Ann. N.Y. Acad. Sci.* **1986**, *484*, 150.
(39) Rupprecht, A.; Kaatze, U. *J. Phys. Chem. A* **1999**, *103*, 6485.